Climate change and nutrient fluctuations interact to affect ecological networks in lakes

Ewa Merz (ewa.merz@eawag.ch)
Eawag, Swiss Federal Institute of Aquatic Science and Technology https://orcid.org/0000-0001-8699-9414

Erik Saberski
University of California, San Diego

Luis J. Gilarranz
Eawag, Swiss Federal Institute of Aquatic Science and Technology

Peter Isles
Vermont Department of Environmental Conservation

George Sugihara
University of California, San Diego

Christine Berger
Stadt Zürich, Wasserversorgung, Qualitätsüberwachung

Francesco Pomati
Eawag, Swiss Federal Institute of Aquatic Science and Technology https://orcid.org/0000-0002-9746-3735

Article

Keywords: climate change, species interactions, connectance, strength, oligotrophication, food webs, trophic controls, bottom-up, top-down, causality, ecological networks

Posted Date: June 30th, 2022

DOI: https://doi.org/10.21203/rs.3.rs-1803809/v1

Abstract

Climate change interacts with local processes to threaten biodiversity by disrupting the complex network of ecological interactions, wherein variation in network links drastically affects ecosystems (e.g., species loss). However, how ecological networks respond to climate change is largely unknown. We herein consider 24–43 years of monthly data from plankton communities in five peri-alpine Swiss lakes subject to warming and re-oligotrophication. Using empirical dynamic modeling, we show that the number and strength of causal taxa interactions respond nonlinearly, yet predictably, to water temperature and phosphorus. Warming reduces the connectance of ecological networks, particularly under high phosphate levels. This network reorganization shifts trophic control of food webs, leading to consumers being controlled by resources—signaling stability loss. By exposing the outcomes of complex interactions between warming, nutrient supply and plankton ecology, our results provide tools for studying and advancing our understanding of how climate change impacts the fabric of biodiversity.

Main Text

Human impacts, such as climate change and pollution, are reorganizing entire ecosystems by affecting the nature and strength of ecological interactions and thereby the composition of communities[1–4]. In fact, the global warming experienced by many lakes, particularly in the last decade, has shifted the balance of these delicate networks to an unstable situation in which slight increases in nutrient levels can trigger dramatic changes[5,6]. If the current rise in temperature continues, as predicted[6], the dynamics of these communities are expected to destabilize[3,7,8]. Recent work suggests that an air temperature increase of 3°C may affect lake water quality similar to the eutrophication of the 20th century[9]. Such a loss of stability can portend the possibility of rapid transitions in ecosystem states and the potential to increase species extinction risks[6,10–12]. Though it is known that human activities affect ecosystems, adapting to a changing climate means we still need better tools for measuring and predicting how changes to any component of the ecosystem shape other components and relative processes[2,13–15].

Ecological interactions between species are the engine of community dynamics and ecosystem processes, though they remain perhaps the most overlooked component of biodiversity change[16,17]. Studying the structure and dynamics of these community interactions, which can be conceptualized as information networks, has proven to be fundamental to understanding how global change alters ecosystem structure and function[18]. Networks vary over space and time in the number of interactions between taxa (i.e., addition or loss of connections, connectance) or in the magnitude (strength) of interactions (i.e., rerouting energy flows through existing connections)[2]. Network connectance and the strength of species interactions—particularly in trophic networks—are structural properties that can signal large-scale changes in the whole ecosystem, with potential implications for system stability and the maintenance of biodiversity[2].

However, knowledge about how entire interaction networks reorganize as a consequence of global change is limited owing to many challenges, including the scarcity of long-term, well-curated time series of complete ecological networks[19], which, when available, are often nonlinear and require specific inference methods[20,21]. Additionally, most research focuses on only one type of interaction (e.g., trophic or competitive). Moreover, until recently, ecological theory and practice have often assumed that interactions are fixed and constant over time[20,22]. Because of the limited available data on large-scale ecosystems and the lack of quantitative data-analytic methods that can address complex relationships that vary with system state, it has been difficult to assess how the properties of ecological networks respond to interacting environmental challenges.

Here, we address these gaps by studying the effects of two major anthropogenic stressors on plankton networks: warming and re-oligotrophication, referring to the process of controlled phosphorus reduction to revert lakes to their original state before anthropogenic nutrient pollution. We measure the temporal changes in connectance and interaction strengths at three levels: (i) the whole network, (ii) top-down and bottom-up links that control food-web dynamics, and (iii) different interaction types. To understand the interdependent effects of warming and oligotrophication on plankton networks, we examined 24–43 years of well-curated monthly plankton community data across five peri-alpine Swiss lakes (Fig. 1a, **Tab. S1**); this dataset is a long-term and consistent historical series of an entire ecological network along with measurements of abiotic environmental variables, which is very rare in ecology. Thus, these data, analyzed via tools for nonlinear dynamic systems, such as empirical dynamic modeling (EDM) (pyedm, rEDM for analyzing non-equilibrium systems) (https://github.com/SugiharaLab), provide a timely opportunity to investigate network-wide consequences of climate change in natural lake ecosystems.

We first analyze the data collected from the five Swiss lakes for the trends in phosphate levels and temperature, as dissolved inorganic phosphorus (phosphate) is the main limiting factor for phytoplankton growth in temperate lakes and the principal driver of eutrophication[23]. Starting in the 1970s, the lakes considered in this study underwent managed re-oligotrophication to control the release of phosphorus into the ecosystems (Fig. 1b). At the same time, the average water column temperature has steadily increased since the 1950s[24], and warming can have both direct and indirect effects on the ecosystems of deep and temperate lakes such as the ones studied here through the regulation of nutrient supply[25]. From 2010–2020, the average water column temperature rose by an alarming 0.6 to 1.8°C (**Tab. S1**), similar to the increase observed over the previous 60 years (1950–2010)[24,26]. This rise in temperature fosters water column stability, reducing turbulence and deep mixing and decreasing the resuspension of phosphorus from the deep and nutrient-rich waters[24,27,28]. To examine these issues, we use a non-linear causality test (convergent cross-mapping, CCM) from the empirical dynamic modeling (EDM) framework to analyze the relationship between phosphate levels and water temperature in our datasets (**Methods**). From this, we find that water column temperature causally influences changes in phosphate levels, but not vice versa **(Fig. S1)**. This unidirectional relationship suggests that warming, by regulating phosphate availability, may have a more pervasive influence on plankton networks than would be expected by the effects of water temperature alone.

To study network connectance, which can be affected by warming[3,29], we next group the plankton species present in the lakes into well-known trophic guilds[16,22,30] based on species' body size, nutrition requirements, and foraging behavior. The resulting conceptual network consists of up to 16 nodes (Fig. 1c, **Methods**) comprising: invertebrate predators, omnivores large and small herbivores, mixotrophic dinoflagellates and primary producers. Guilds of primary producers (phytoplankton) represent the base of aquatic food webs and, worldwide, they account for half of the global primary production[31]. We divided each of their guilds into two nodes based on cell size and coloniality (Fig. 1c). Each node in the network contains a time series of monthly abundances that records how guilds wax and wane over time, while the number of nodes per lake remains constant (**Fig. S2**, **Fig. S3**). These time series contain essential information about how the nodes influence each other (i.e., dynamic links). We consider direct (e.g., predator-prey) and indirect (e.g., competition for resources) interactions.

To employ this established network for studying how interactions change as a function of system state (as reasonably expected from nonlinear systems[20,32]), we use EDM to recover and analyze the putative attractor that generated the observational time series. We quantify the strength of causal associations between network nodes using CCM and Pearson's correlation between predictions and observations (rho, cross-map accuracy)[32]. CCM quantifies how changes in one time series (the driven variable) can predict changes in another (the causal driver). That is, it quantifies how much information about the driver is contained in the driven variable. Of note, with CCM, we can detect nonlinear linkages between nodes that show no correlation with each other or whose ephemeral correlations can flip signs—a common phenomenon in nonlinear systems. Causal interactions between two network nodes are tested in both directions (e.g., from prey to a predator and from predator to its prey). To highlight the intrinsic nonlinear dynamics among the guilds and minimize the interannual signal of the environmental drivers, interactions are corrected for seasonality by assuming no interaction when the interaction strength given by CCM is lower than that of a seasonal surrogate null model[33,34] (**Methods**). By measuring cross-map accuracy (rho) in a 60-month moving window, we track how the strength of causal influence between plankton guilds varies. Thus, within each window, we calculate a CCM network and measure (i) connectance as the percentage of significant causal links between guilds (nodes), $C = 100 \times (L / N(N-1))$, where L is the number of interactions between nodes and N is the number of nodes in the system, and (ii) interaction strengths among causal links. The main trends in connectance and interaction strength reported below are robust to the choice of window size (**Fig. S4**).

At the network level, we find that connectance and average interaction strengths vary over time in each lake (Fig. 2a-b**)**. Plankton network connectance increases across lakes as nutrient availability decreases; then drops sharply after 2010 (from an average connectance of 24% realized links to 10%) as warming accelerates (Fig. 2a). The average interaction strength among plankton guilds is less variable over time than network connectance, with a slight temporal decrease after re-oligotrophication (Fig. 2b).

To then examine the relationship between network properties and environmental factors, we study the effects of contrasting gradients of decreasing phosphorus and lake warming experienced by all the lakes

in our dataset (Fig. 1b). Using s-maps (**Methods**), we model the highly non-linear relationship between network properties as a function of the interaction between temperature, phosphate, and the lake's depth and volume[23,35]. Those models allow us to examine the effects of warming, usually convolved with re-oligotrophication, as a function of lake size. Moreover, within the observed ranges of temperature and phosphate levels, we can now make out-of-sample predictions for previously unobserved temperature and phosphate level combinations across lakes.

We found that network connectance and interaction strength show non-linear responses to changes in lake phosphate concentration and water temperature (Fig. 2c-d). Here, the degree of nonlinearity is measured by the maximum Δrho: the difference in Pearson's correlation between the best nonlinear model (when the locality parameter [Θ] in the s-maps is greater than 0) and the global linear model (when Θ = 0) (**Tab. S2**). Though dependent on temperature and lake size, overall the connectance and interaction strength increase with decreasing phosphorus levels in the S-map models. However, the observed historical trajectories show that network connectance responds idiosyncratically when phosphate levels decrease, tending to increase in large lakes and decrease in small (+ 8.0%, -6.7%, respectively; Fig. 2c). When water temperature and phosphate levels remain relatively stable, connectance increases in small and large lakes (+ 14.8%, + 9.3%; Fig. 2c). Finally, connectance drastically decreases when warming accelerates (-15.8.%, -12.1%; Fig. 2c). S-map models predict network connectance to be highest at moderate to low temperature and low phosphate levels ($T < 8.12°C$, $P < 0.03$ mg/L), though connectance is consistently lower in both small and large lakes at high temperature, irrespective of phosphate levels ($T > 8.83°C$, $P > 0.03$ mg/L; Fig. 2c). Our results here, showing significantly reduced connectance across different lake ecosystems with increasing water temperature, especially under eutrophic conditions, agree with recent evidence from natural freshwater systems[3] that warming reduces the connectance of natural ecological networks.

Regarding interaction strength, we see that a decrease in phosphorus is a stronger driver than water temperature. S-map models predict network interactions to be generally stronger under low phosphate levels ($P < 0.03$ mg/L) and weaker at low temperatures and high phosphate levels ($T < 7.23°C$, $P > 0.11$ mg/L, Fig. 2d). Moreover, the strength of network interactions in smaller lakes is predicted to be higher and more dynamic on average when compared to larger lakes (0.44 ± 0.06, 0.31 ± 0.02, respectively; Fig. 2d). Overall, stable ecosystems are characterized by high connectivity and weak interaction strengths[7], and a reduction in nutrient levels can increase competition for resources and thus lead to stronger interactions[36,37]. Our models predict that stable conditions are satisfied in our dataset under low to intermediate water temperatures, implying that the warming of temperate lakes might destabilize plankton networks, particularly when interacting with very high phosphorus levels, as previously suggested[5].

We next examined the directionality of trophic control, as warming can alter the metabolic rates of producers and consumers differently, influencing the strength of trophic interactions and the direction of controls (e.g. consumers controlling the population of their resource or vice versa), especially under

reduced nutrient levels[3,5,38]. Experimental evidence suggests that warming strongly impacts aquatic food web interactions by reducing trophic transfer efficiency[38–40] and may also affect trophic controls in large lakes, particularly when co-occurring with changes in nutrient availability[4,25,41]. If warming shifts control to bottom-up, where resources control consumers, the system dynamics become sensitive to nutrient inputs[5,42]. If top-down forces control a system, managing the lake's productivity would require food web manipulations (e.g., stocking of piscivorous fish)[43]. When ecosystems depend on resources to meet consumers' demands, they also become significantly destabilized[3].

To therefore explore the directionality of trophic control, we use CCM to calculate the relative frequency of causal effects descending (top-down links, e.g. predator controls prey abundance), and ascending (bottom-up links, e.g. prey controls predator abundance) the network (Fig. 1c, **Methods**). To reveal the complex responses of bottom-up and top-down controls to phosphate concentration and warming, we use s-maps models analogous to those used to predict connectance and interaction strength. We find that top-down causal links are more frequent than bottom-up links in all lakes (Fig. 3a, **Fig. S6a**), though in 4 out of 5 lakes, the bottom-up links are stronger on average (Fig. 3b). Additionally, bottom-up and top-down controls are not static and change over time and environmental gradients[4]. We find that, across lakes, a reduction in phosphate levels slightly increases the number of top-down links (Fig. 3c). Warming in lakes, however, generally decreases both the number and strength of top-down links relative to bottom-up links (Fig. 3c-d). Our s-map models predict that under high water temperature and high phosphate levels, plankton networks are bottom-up controlled (number and strength of links, $T > 8.00°C$, $PO_4 > 0.025$ mg/L), whereas they are top-down controlled under low water temperature and low nutrients ($T < 8.00°C$, $PO_4 < 0.025$ mg/L; Fig. 3c-d). Although combined warming and nutrient levels can have system-specific and idiosyncratic shifts in bottom-up and top-down controls[5,42], our results suggest that under warming conditions, resources increasingly control consumers in planktonic food webs, particularly when phosphorus levels are high.

So far, our results have shown how plankton networks respond to changes in temperature and phosphate concentration. To better understand the mechanisms leading to the observed network reorganization, we examine how different interaction types and guilds contribute to the temporal changes in connectance, interaction strength, and trophic controls. We obtain the frequency and average strength of trophic, non-trophic, and hybrid links, the latter of which can be both trophic and non-trophic depending on the conditions (e.g., mixotrophic dinoflagellates that change nutrition mode, or links involving large zooplankton that both prey on and compete with microzooplankton like rotifers and ciliates). The temporal dynamics show that hybrid links are significantly more common in the causal network than non-trophic and trophic links, especially after 2010 (Fig. 4a, Fig. 4c). Trophic (e.g., predator-prey interactions) and non-trophic links (e.g., competition and facilitation) were similarly frequent across lakes ($p = 0.26$, Fig. 4c), though non-trophic links were strongest on average, especially before nutrient stabilization in the systems ($p < 0.001$; Fig. 4b,d), while trophic and hybrid links had similar strengths ($p = 0.31$; Fig. 4d). These results suggest that hybrid links are important regulators of plankton network structure, as previously hypothesized[2].

By shifting our focus from interactions to the constituent nodes, we find that temperature and phosphate availability have a strong causal influence on specific guilds: small grazers (i.e., rotifers, ciliates and mixotrophic dinoflagellates; guilds R, Ci, and M) and colonial cyanobacteria (P2) (Fig. 5). These guilds lead the responses of plankton networks to warming and re-oligotrophication as they have the strongest influence on the dynamics of other guilds (Fig. 5). Mixotrophic dinoflagellates account for most of the top-down links (**Fig. S6b**), while ciliates have the strongest top-down links, followed by rotifers and mixotrophic dinoflagellates (**Fig. S6c**). These findings agree with previous knowledge of mixotrophic organisms and small grazers being more resilient to environmental change due to their plastic nutrition strategies and foraging behavior. As a central regulator of plankton food webs[30,44], they influence community structure[35] and food web dynamics[2]. Colonial, bloom-forming (and often toxic) cyanobacteria are among the most frequent and strongest linked primary producers in our plankton networks (Fig. 5 and S6). As expected, the dynamics of cyanobacteria are strongly linked to changes in phosphate levels and temperature[45] (Fig. 5). While their connectivity and interaction strengths decrease with re-oligotrophication, the strength of their interactions increases with warming (**Fig. S7**).

The results we present here provide much-needed information about how lake plankton interaction networks, which are paramount for the functioning of aquatic ecosystems, respond to climate change and pollution, and characterize their highly nonlinear behavior. These results also highlight the necessity for studies of this type, as we show that the warming experienced by the lakes in this dataset, particularly in the last decade, has shifted network properties and trophic controls to an area of parameter space where slight increases in temperature or phosphorus levels can trigger dramatic changes in the network (Figs. 2–3, S5). Given the high stakes for biodiversity and water security, it is essential to develop the capacity to forecast future lake ecosystem states, and to allow conservation and management by exploring outcomes under different climate scenarios. The tools used here will enable us to measure and predict the complex relationships between network properties, climate change, and nutrient supply. With adequate data, we are now in a position where ecological forecasting is feasible, not only in lakes but in other systems where data-driven modeling tools similar to those used here can be applied by researchers and stakeholders alike.

Declarations

Author Contributions

E.M., F.P., L.J.G. and P.I. initiated the study, all authors contributed to its design. C.B. collected the data (for lake Zurich). E.M. assembled the data and E.M., E.S. performed analyses. E.M., L.J.G., F.P., E.S. and G.S. drafted the manuscript; all authors provided critical feedback (contributing roles based on https://casrai.org/credit/).

Acknowledgments

We thank Marta Reyes (expertise in plankton taxonomy), Thea Bulas and Ester (zooplankton counts GRE), Silvana Käser (phytoplankton counts GRE), Hansruedi Bürgi (plankton counts GRE, HAL, BAL, SEM), Michael Koss and Oliver Köster (ZHR data), Stefanie Merkli (AWEL), Lukas de Ventura (HAL data), Robert Lovas (BAL, SEM data), and Owen Petchey and Ignacio Perez-Dominguez (feedback on the manuscript). This research was funded by the Swiss National Science Foundation (project 182124). F.P. and P. I. also acknowledge the Eawag DF project Cyanoswiss (#5221.00492.012.04). L.J.G. was supported by the Swiss National Science Foundation Ambizione Fellowship (PZ00P3_185951). E.S. and G.S. acknowledge the DoD-Strategic Environmental Research and Development Program (15 RC-2509), the National Science Foundation (DEB-1655203 and ABI-1667584), the Department of Interior (NPS-P20AC00527), the McQuown Fund and the McQuown Chair in Natural Sciences, University of California, San Diego.

References

1. Estes, J. A. *et al.* Trophic downgrading of planet Earth. *Science* **333**, 301–306 (2011).

2. Bartley, T. J. *et al.* Food web rewiring in a changing world. *Nat Ecol Evol* **3**, 345–354 (2019).

3. O'Gorman, E. J. *et al.* A simple model predicts how warming simplifies wild food webs. *Nat. Clim. Chang.* **9**, 611–616 (2019).

4. Rogers, T. L. *et al.* Trophic control changes with season and nutrient loading in lakes. *Ecol. Lett.* **23**, 1287–1297 (2020).

5. O'Connor, M. I., Piehler, M. F., Leech, D. M., Anton, A. & Bruno, J. F. Warming and resource availability shift food web structure and metabolism. *PLoS Biol.* **7**, e1000178 (2009).

6. Kraemer, B. M. *et al.* Climate change drives widespread shifts in lake thermal habitat. *Nature Climate Change* vol. 11 521–529 (2021).

7. Timothy Wootton, J. & Emmerson, M. Measurement of Interaction Strength in Nature. (2005) doi:10.1146/annurev.ecolsys.36.091704.175535.

8. Grilli, J., Barabás, G., Michalska-Smith, M. J. & Allesina, S. Higher-order interactions stabilize dynamics in competitive network models. *Nature* **548**, 210–213 (2017).

9. Ethan Deyle, Damien Bouffard, Victor Frossard, Robert Schwefel, John Melack, George Sugihara. A hybrid empirical and parametric approach for managing ecosystem complexity: water quality in Lake Geneva under nonstationary futures. *Proc. Natl. Acad. Sci. U. S. A.* in press (2022).

10. Dunne, J. A., Williams, R. J. & Martinez, N. D. Network structure and biodiversity loss in food webs: robustness increases with connectance. *Ecol. Lett.* **5**, 558–567 (2002).

11. Gilbert, A. J. Connectance indicates the robustness of food webs when subjected to species loss. *Ecol. Indic.* **9**, 72–80 (2009).

12. Scheffer, M. *et al.* Early-warning signals for critical transitions. *Nature* **461**, 53–59 (2009).

13. Cardinale, B. J. *et al.* Biodiversity loss and its impact on humanity. *Nature* **486**, 59–67 (2012).

14. Trisos, C. H., Merow, C. & Pigot, A. L. The projected timing of abrupt ecological disruption from climate change. *Nature* vol. 580 496–501 (2020).

15. Chang, C.-W. *et al.* Long-term warming destabilizes aquatic ecosystems through weakening biodiversity-mediated causal networks. *Glob. Chang. Biol.* **26**, 6413–6423 (2020).

16. Poisot, T., Stouffer, D. B. & Gravel, D. Beyond species: why ecological interaction networks vary through space and time. *Oikos* **124**, 243–251 (2015).

17. Valiente-Banuet, A. *et al.* Beyond species loss: the extinction of ecological interactions in a changing world. *Funct. Ecol.* **29**, 299–307 (2015).

18. Montoya, J. M. & Raffaelli, D. Climate change, biotic interactions and ecosystem services. *Philos. Trans. R. Soc. Lond. B Biol. Sci.* **365**, 2013–2018 (2010).

19. Dornelas, M. *et al.* BioTIME: A database of biodiversity time series for the Anthropocene. *Glob. Ecol. Biogeogr.* **27**, 760–786 (2018).

20. Deyle, E. R., May, R. M., Munch, S. B. & Sugihara, G. Tracking and forecasting ecosystem interactions in real time. *Proc. Biol. Sci.* **283**, (2016).

21. Runge, J. *et al.* Inferring causation from time series in Earth system sciences. *Nat. Commun.* **10**, 1–13 (2019).

22. Ushio, M. *et al.* Fluctuating interaction network and time-varying stability of a natural fish community. *Nature* **554**, 360–363 (2018).

23. Jeppesen, E. *et al.* Lake responses to reduced nutrient loading - an analysis of contemporary long-term data from 35 case studies. *Freshw. Biol.* **50**, 1747–1771 (2005).

24. Livingstone, D. M. Impact of secular climate change on the thermal structure of a large temperate central European lake. *Clim. Change* **57**, 205–225 (2003).

25. Anneville, O. *et al.* The paradox of re-oligotrophication: the role of bottom–up versus top–down controls on the phytoplankton community. *Oikos* **128**, 1666–1677 (2019).

26. Pomati, F., Matthews, B., Jokela, J., Schildknecht, A. & Ibelings, B. W. Effects of re-oligotrophication and climate warming on plankton richness and community stability in a deep mesotrophic lake. *Oikos* **121**, 1317–1327 (2012).

27. Posch, T., Köster, O., Salcher, M. M. & Pernthaler, J. Harmful filamentous cyanobacteria favoured by reduced water turnover with lake warming. *Nat. Clim. Chang.* **2**, 809–813 (2012).

28. Winder, M. & Sommer, U. Phytoplankton response to a changing climate. *Hydrobiologia* **698**, 5–16 (2012).

29. Petchey, O. L., Brose, U. & Rall, B. C. Predicting the effects of temperature on food web connectance. *Philos. Trans. R. Soc. Lond. B Biol. Sci.* **365**, 2081–2091 (2010).

30. Ehrlich, E. & Gaedke, U. Coupled changes in traits and biomasses cascading through a tritrophic plankton food web. *Limnol. Oceanogr.* **65**, 2502–2514 (2020).

31. Falkowski, P. Ocean Science: The power of plankton. *Nature* **483**, S17–20 (2012).

32. Sugihara, G. *et al.* Detecting causality in complex ecosystems. *Science* **338**, 496–500 (2012).

33. Deyle, E. R., Maher, M. C., Hernandez, R. D., Basu, S. & Sugihara, G. Global environmental drivers of influenza. *Proc. Natl. Acad. Sci. U. S. A.* **113**, 13081–13086 (2016).

34. Sugihara, G., Deyle, E. R. & Ye, H. Reply to Baskerville and Cobey: Misconceptions about causation with synchrony and seasonal drivers. *Proceedings of the National Academy of Sciences of the United States of America* vol. 114 E2272–E2274 (2017).

35. Pomati, F., Shurin, J. B., Andersen, K. H., Tellenbach, C. & Barton, A. D. Interacting Temperature, Nutrients and Zooplankton Grazing Control Phytoplankton Size-Abundance Relationships in Eight Swiss Lakes. *Front. Microbiol.* **10**, 3155 (2019).

36. Litchman, E., Edwards, K. F. & Klausmeier, C. A. Microbial resource utilization traits and trade-offs: implications for community structure, functioning, and biogeochemical impacts at present and in the future. *Front. Microbiol.* **6**, 254 (2015).

37. Ehrenfels, B. *et al.* Diazotrophic Cyanobacteria are Associated With a Low Nitrate Resupply to Surface Waters in Lake Tanganyika. *Front. Environ. Sci. Eng. China* **9**, 277 (2021).

38. Barneche, D. R. *et al.* Warming impairs trophic transfer efficiency in a long-term field experiment. *Nature* **592**, 76–79 (2021).

39. Petchey, O. L., McPhearson, P. T., Casey, T. M. & Morin, P. J. Environmental warming alters food-web structure and ecosystem function. *Nature* **402**, 69–72 (1999).

40. Murphy, G. E. P., Romanuk, T. N. & Worm, B. Cascading effects of climate change on plankton community structure. *Ecol. Evol.* **10**, 2170–2181 (2020).

41. Frossard, V., Rimet, F. & Perga, M.-E. Causal networks reveal the dominance of bottom-up interactions in large, deep lakes. *Ecol. Modell.* **368**, 136–146 (2018).

42. Shurin, J. B., Clasen, J. L., Greig, H. S., Kratina, P. & Thompson, P. L. Warming shifts top-down and bottom-up control of pond food web structure and function. *Philos. Trans. R. Soc. Lond. B Biol. Sci.* **367**, 3008–3017 (2012).

43. Carpenter, S. R., Kitchell, J. F. & Hodgson, J. R. Cascading Trophic Interactions and Lake Productivity. *Bioscience* **35**, 634–639 (1985).

44. Boit, A., Martinez, N. D., Williams, R. J. & Gaedke, U. Mechanistic theory and modelling of complex food-web dynamics in Lake Constance. *Ecol. Lett.* **15**, 594–602 (2012).

45. Huisman, J. *et al.* Cyanobacterial blooms. *Nat. Rev. Microbiol.* **16**, 471–483 (2018).

Methods

Data collection

Plankton abundance time series covering three levels of a lake's food web

Plankton samples were collected between 1977 and 2020 monthly (occasionally bi-monthly) across 5 Swiss lakes (**Fig. 1, Tab. S1**). In Lake Baldegg and Sempach, data from 2010 onwards were excluded from analyses due to irregular plankton sampling (i.e., bi- or tri-monthly). Samples in all lakes have been collected at identical locations over the years and were counted by the same group of taxonomists. Phytoplankton and small zooplankton grazers (i.e., rotifers and ciliates) were sampled integrated over the water column using a Schröder sampler [46] or at discrete depths, where the lowest depth varied across lakes. Taxa abundances were converted to cells/L to compare across lakes. In Zurichsee, the sampling method was changed in 2012 from discrete depth sampling (0, 1, 2.5, 5, 7.5, 10, 12.5, 15, 20, 30, 40, 60, 80, 100, 120, 130, 135 m) to integrated sampling (<20 m, 20-40 m and >40 m of the water column). To compare discrete with integrated samples, we multiplied each discrete sample by a conversion factor and aggregated them to match the corresponding integrated samples, e.g. multiplied discrete samples within 0 to 20 m by their corresponding factor and summed them up to match the integrated samples of < 20 m. Conversion factors for the specific depths can be found on an open data repository linked to this article (**link to ERIC server)**. Zurichsee (ZHR) sampling did not consider small grazers (ciliates and rotifers). Large zooplankton was sampled using net-tows going from the bottom of the lake to the surface. Details about the lake sampling protocols can be found elsewhere [26,35]. Densities were converted to individuals/m2 to compare across lakes. A full taxonomic list of species considered within this study can be found in an open access data repository linked to this article (**link to ERIC server**). Plankton abundance data were winsorized, where values lying outside the 99 % quantile were replaced by the highest values within the 99 % quantile using the function **Winsorize** from the R package **DescTools** (**v 0.99.43**). This was done to reduce the power of large outliers without deleting data.

Water temperature and nutrient availability as environmental drivers

Chemical and physical parameters were measured monthly (occasionally bi-monthly) in the same locations where plankton samples were collected. Samples were done from the surface to the lake's bottom at discrete depths. We focused on two main drivers of anthropogenic change in Swiss lakes, water temperature and freely available dissolved phosphate (PO_4) [47,48]. We used mean water temperature and mean phosphate concentration over the whole water column. Missing values were estimated using linear interpolation with **na_approx** from the R package **zoo (v 1.8-9)**. The approximated values ranged between 1 and 218, with a median of 2.5 (**Tab. S1**). After re-oligotrophication, PO_4 levels remained constant and often below the detection limit in Lake Hallwil. Sampling for nutrients in this lake was changed to bi- or tri-monthly early on in 1988, resulting in 218 missing values.

Conceptual planktonic network

To understand processes at the network level and control for potential biases in taxa classification across lakes and over time, we aggregated plankton taxa abundances into a conceptual network. This allowed us to overcome the limitations of a monitoring frequency lower than the generation time of the organisms (monthly sampling and noise in time series), and account for the intrinsic variability of species interactions. We aggregated taxa into guilds based on functional traits allows to reduce the potential effects of taxonomic misclassification [49], and the dynamics of trophic guilds, contrary to the dynamics of taxa (which occur at the scale of days), occur at the scale of months and well represent seasonal and interannual network transitions [30,44].

The sorting into guilds and drawing links between them was based on taxonomic classification, body size, and feeding behavior [44]. Our conceptual network consisted of up to 16 nodes (guilds) across three trophic levels of the food web, containing large invertebrate predators, omnivores, large herbivore grazers, small grazers, mixotrophs, and primary producers. The relationships (links) between nodes can be trophic (classic predator-prey relationship), non-trophic (i.e., mutualisms and competition) or hybrid, where guilds can have trophic or non-trophic relationships (i.e., mixotrophic dinoflagellates) (**Fig. 1c**). All links are bi-directional (in both directions), whereas trophic and hybrid links can go up the network (BU), i.e., from a primary producer to a grazer, or down the network (top-down), i.e., from a grazer to a primary producer (**Fig. 1c**). We sorted in total 1383 distinctive taxa into 16 guilds. In Zurichsee, we only had 14 guilds because of missing counts for rotifers and ciliates. We conducted a sensitivity analysis where we excluded rotifers (R) and ciliates (Ci) from Greifensee data. Connectance and interaction strength were similar with and without rotifers (R) and ciliates (Ci) ($R^2_{connectance} = 0.92$, $p\text{-value}_{connectance} < 2.2\ e^{-16}$, $R^2_{interaction\ strength} = 0.79$, $p\text{-value}_{interaction\ strength} < 2.2\ e^{-16}$). Because we could not differentiate between calanoid and cyclopoid nauplii nor their larval stage and thus had not enough information on their feeding behavior, nauplii were excluded from our study. Euglenoids were also excluded. An overview of the taxonomic list and guild classification can be found in an open access data repository linked to this article (**link to ERIC server**). The guild abundances for each lake, as shown in **Fig. S2** are freely available and can be downloaded here (**link to ERIC server**) after the manuscript submission.

For analyses, time series were completed by adding a placeholder for missing values (NA's) to ensure having evenly spaced monthly data. If guilds did not meet a 50% abundance criteria, i.e., present (values greater than 0) at least half of the time during the studied period, they were excluded from the analysis. This has been the case for P1 (small cyanobacteria) in HAL, BAL, SEM and ZHR.

Empirical Dynamic Modeling (EDM)

Chaos is ubiquitous in plankton communities, making linear statistical approaches unfit to study long-term changes in their network properties [50]**.** Linear statistical techniques are based on a correlation between two or more variables. In nonlinear systems, causality does not require correlation and correlation does not imply causation [32]. Nonlinear systems can exhibit state dependency, where the relationships between variables may change depending on the system's state. For example, large herbivore populations (**H**) may be affected by invertebrate predators (**C2**) only when their resource, phytoplankton (**P**), is scarce [51]. Equation-free approaches offer a promising way to detect causal relationships in complex non-linear systems.

Empirical dynamic modeling (EDM) is rooted in state-space reconstruction, which does not assume any equations governing the system and recovers dynamics from empirical data. In EDM, a state space (i.e., an attractor) is reconstructed using time series belonging to the same dynamical system. An attractor is a description of rules that govern the system - without any a priori assumptions. For example, suppose the dynamics of large herbivores (**H**) are affected by phytoplankton (**P**) and invertebrate predators (**C2**). In that case, an attractor of the system's dynamics can be reconstructed by plotting the time series of **H**, **P** and **C2** along the x,y, and z axes. An educative animation on state-space reconstruction can be found here: https://deepeco.ucsd.edu/videos/#page-content.

In practice, we typically don't have knowledge of or data on every variable in a system. Takens' Theorem (1981), however, postulated that one can substitute any unknown or unobserved variables with a lag of a single time series to reconstruct the system's attractor [52]. If two variables are from the same dynamical system, i.e. large herbivores (**H**) and phytoplankton (**P**), information about current phytoplankton populations will be encoded in past large herbivores' time series. Thus, if we have no information on phytoplankton (**P**) and invertebrate predators (**C2**), the system from above can be reconstructed using large herbivore abundance (**H**) at **t-τ** and **H** abundance at **t-2τ** respectively, where **τ** stands for time lag (e.g. 1 month).

To reconstruct the attractor of a system properly, one needs to know the ideal embedding. The ideal embedding is defined by the number of variables or lags used to build a system's attractor, each of them representing a coordinate axis; and provides information on the complexity of the system and the quality of data (i.e. highly resolved time series contain more information on the system and will thus result in a higher ideal embedding dimension). In our example above, the embedding dimension was set arbitrarily to three and a shadow attractor was reconstructed using large herbivore abundance (**H**) at **t**, **t-τ** and **t-2τ**. Ideally, we would define the best embedding first and then reconstruct the attractor using (**H(t), H(t-τ), H(t-**

2τ), …, H(t-(E)τ), where **τ** is the desired lag (i.e. one month) and **E** the best embedding (see below for further explications).

In empirical dynamic modeling, the attractor of a system can be used (among others) to determine the number of dimensions required to describe a system (best embedding) [53,54], quantify the non-linearity of time series [55–57], forecasting [53,58–60] and infer causality between two variables [32]. We expanded the classical empirical dynamical framework by adding a temporal component to convergent cross mapping (studying local correlations among observations and predictions within a moving window) and using the predictive skill rho (corrected for seasonality) as a proxy for how strongly a variable interacts and/or affects another variable. Below we briefly introduce the EDM concepts used in this paper and how we applied them to our data. Please refer to the cited references for proof of concepts and further information.

Before analysis using empirical dynamical modeling, guild time series have been rescaled using the function **scale** in the R package **base** (**v-4.1.0**). All analyses were performed using the **rEDM** package in R **(v-0.7.5)**. Up-to-date versions of rEDM can be found at https://github.com/SugiharaLab/rEDM. More information to perform EDM analyses can be found here: https://deepeco.ucsd.edu/resources/#page-content. “Empirical dynamic modeling for beginners” is another helpful resource, addressing basic applications with step-by-step example code [61].

Optimal Embedding Dimension

To reconstruct the dynamic attractor, one needs to know the ideal embedding dimension, i.e. the number of independent variables. The ideal embedding can be defined with simplex projection, a forecasting method relying on nearest neighbors [53]. Simplex projection uses only neighboring points in the state space of the predicted variable to make forecasts. The highest prediction skill (rho, Pearson’s correlation ρ between the observed and the predicted values) indicates the optimal embedding dimension. If the right number of lags are used, the attractor reconstruction will map closely to that of the true underlying attractor of the system. If embeddings are insufficient, points corresponding to different system states will overlap in the reconstruction and thus hinder forecast accuracy.

We used **simplex** from the R package **rEDM** (**v-0.7.5)** to perform simplex projection and define the best embedding dimension for each time series in our data. The embedding dimension was run over E = 2:15. Time lag and prediction horizon were set to 1 month. The number of nearest neighbors used to make predictions was set to E+1. Forecasting was done using leave-one-out cross-validation and the best embedding was selected based on maximizing the forecasting skill rho (**Tab. S2)**.

Non-linearity

EDM was designed for non-linear deterministic systems, an assumption that must be tested before analysis. The degree of state dependency reflects the nonlinearity of a system. State dependency, and thus the degree of non-linearity, can be determined using univariate s-maps forecasting (s-map stands for

sequential locally weighted global linear map)[55]. S-maps use the whole library of points to make forecasts and apply a weighting function (e.g. in the form of an exponential decay kernel), giving closer points in attractor space more weight. The non-linear tuning parameter theta controls the state dependency in the weighting function of an s-map. If theta = 0, all library points receive the same weight and thus, the system is considered linear. In that case, the model reduces to a linear autoregressive model. However, nearby points receive larger weights if theta is greater than 0. The s-map forecasting will depend on the system's local state. It will produce different fittings depending on the position along the attractor. The larger theta, the more weight is given to closer points (neighbors) in the attractor space for forecasting. Nonlinearity can be explored by comparing the forecasting skill of linear (theta = 0) to nonlinear models (theta > 0).

We used **s_map** from the R package **rEDM** (**v-0.7.5)** to quantify the degree of nonlinearity (theta) for each time series in our data set. Embedding was fixed depending on the previously defined best embedding dimension (**Tab. S3**) and theta run over a list of values (0, 0.0001, 0.0003, 0.001, 0.003, 0.01, 0.03, 0.1, 0.3, 0.5, 0.75, 1.0, 1.5, 2, 3, 4, 6, and 8). Time lag and prediction horizon were set to 1 month. Forecasting was made using leave-one-out cross-validation and theta was selected based on maximized forecasting skill rho (**Tab. S3)**.

Convergent Cross Mapping

Convergent cross-mapping (CCM) is considered a "non-linear causality test" and assesses if one variable significantly affects another. As a consequence of Taken's theorem, univariate attractor reconstructions map to the original system and each other. By testing for mapping between two univariate attractor reconstructions, we can determine if two variables belong to the same system and thus share a causal relationship [32]. If large herbivores (**H**), phytoplankton (**P**) and invertebrate predators (**C2**) belong to the same system (are causally linked) and the best embedding is 3, the attractor (**H(t), H(t-τ), H(t-2τ)**) maps to the attractor (**H(t), P(t), C2(t)**) as well as (**P(t), P(t-τ), P(t-2τ)**) and (**C2(t), C2(t-τ), C2(t-2τ)**). In practice, this is done by testing how well a variable can be predicted using another variable's attractor reconstruction. We measure the forecasting skill rho (Pearson's correlation between predictions and observations), also called the "cross-mapping skill". For example, we may use the univariate reconstructed attractor (**P(t), P(t-τ), P(t-2τ)**) based on phytoplankton (**P**) to predict large herbivore abundance (**H**) at **t** or **t-τ**. Note that some causal relationships may be unidirectional, e.g., temperature will map to large herbivores (**H**) but not vice versa.

Convergence and surrogate time series are critical components of inferring causality between two variables using empirical data. Cross-mapping from one variable to another shall be "convergent", i.e., the predictive skill rho improves with library size (time-series length). Reconstructed univariate attractors become denser with more library points and thus, forecasts using nearest neighbors become better. The state space is reconstructed using different library lengths (number of data points) subsampled randomly from the time series to test for convergence. Seasonal co-occurrence patterns might obscure a causal relationship of one variable to another, which is especially true for plankton communities (i.e. PEG model

[62]. Two variables with a seasonal cycle can have a high prediction skill, even if they don't share a causal link. Therefore, one can compare the forecasting skill rho of the original time series to rho estimated from seasonal surrogates. Seasonal surrogate time series are created by randomly reshuffling the time series while keeping the seasonal signal (i.e., reshuffling among months).

Local cross-mapping skills (rho) describe changes in significant links over time and can be used to estimate time-varying (interaction) strength. Cross-mapping-skill is usually calculated over the whole time series. Local cross-mapping skills document changes in (plankton) networks and aid in overcoming a common trend. Instead of calculating Pearson's correlation between all observations and predictions, cross-mapping skills are estimated within a moving window. This results in a time series of cross-mapping skills, which can be used to derive time-dependent causal links when compared to seasonal surrogate time series. The local cross-mapping skill can be used as a proxy for the strength of the causal link when subtracting the seasonal component (i.e., $rho_{originalTS}$ - mean ($rho_{surrogateTS}$)). If this is done for a link between two network nodes, i.e., phytoplankton (P) and large herbivores (H), local cross-mapping skills can be used as a proxy for interaction strength between those two nodes.

In the following two paragraphs, we will briefly describe how we used convergent cross-mapping to derive time-dependent causal links and estimate the strength of those causal links. Consider two variables, V1 and V2. We want to know if V1 (e.g., phytoplankton) had a significant link with V2 (e.g., large herbivores or temperature) at time point t_x and how strong the link was. To do this, we would call it V1 xmap V2 and the direction of effect we are testing is V1 ← V2.

Convergence test. We tested the convergence of V1 xmap V2 by comparing the predictive power of using 20% and 50% of the data, respectively. This was done with 100 consecutive random subsets of the time series. The ideal embedding dimension was defined for V1 based on forecasting with simplex-projection (see above and **STab. 2**), while the time lag tp was kept at 0. Convergent cross mapping was run with the function **ccm** from the R package **rEDM** (**v-0.7.5**). Convergence was considered true if $rho_{50\%} > rho_{20\%}$ for the 100 subsets, determined by a one-sided t-test (95% quantile). **Local cross-mapping-skill (rho).** If the convergence test was significant, we performed CCM between V1 and V2 this time using the maximum library (whole time series) and tp = -1. Using the predictions from the CCM-output, we calculated local rho's, i.e. the correlation between observation of V1 and predictions of V1 (using V2's attractor) within moving windows (n=60 months, sliding 1 month forward at a time). This resulted in a time series of rho's (forecast skills). **Seasonal surrogates.** The local rho's were then compared to rho's from 100 random seasonal surrogate time series for each time window (time point t_x). **Causal link.** We considered the link V1 ← V2 at time point t_x as significant if 95% of the times $rho_{originalTS} > rho_{surrogateTS}$. **Strength.** If the link was significant, we estimate the strength of V1 ← V2 at t_x by removing the seasonal component from the local $rho_{originalTS}$, i.e. $rho_{originalTS}$ - mean ($rho_{surrogateTS}$), the average local rho of the 100 surrogate time series.

Network links. To calculate network connectance, we summed all causal links (passed the surrogate test) per lake and date (month) and divided them by the total possible links for this network (based on the

conceptual network and convergence test). We obtained connectance (%), the number of connected nodes, for this time point and a time series of connectance per lake (**Fig. 2a**). **Interaction strength.** We calculate the mean interaction strength (correlation between observed and predicted values) across nodes per date and lake. This resulted in average interaction strength for this time point and a time series of average interaction strength per lake (**Fig. 2b**). If there were no significant links at a given time point, connectance was set to 0 and strength to NA. Interaction strength over time and across lakes (**Fig. 5**) was calculated by estimating the average strength of each link and multiplying it by its prevalence over time (per lake), i.e. corrected the strength for how often it occurred in the time series, and then average across lakes. **Environment effect on guilds.** To get at the strength of water temperature and phosphate variability over time for each guild (**Fig.5**), we averaged the strength for each node and multiplied by its prevalence over time and then averaged across lakes (analogous to calculating interaction strengths between guilds over time across lakes). **Feedback between temperature and nutrients.** To test for a causal relationship (feedback) between water temperature and phosphate concentration (**Fig. S1**), we used convergent cross-mapping on the whole time series and performed a convergence test (n=100) and seasonal surrogate test (n=100). If both the convergence test ($rho_{50\%} > rho_{20\%}$) and seasonal surrogate test (>95% of times $rho_{originalTS} > rho_{surrogateTS}$) passed, we considered an effect as significant (lake displayed as points in **Fig. S1**). To get a robust estimation of the effect's magnitude (i.e. filter out single episodic events and diminish the power of outliers), we multiplied the strength of each time point by its prevalence over time (per lake), i.e. we corrected the strength by how often a significant link occurred in the time series. The resulting value was plotted on the y-axis in **Fig. S1**. **Network control.** We summed up all causal links going up (bottom-up) and down (top-down) the food web (i.e., trophic and hybrid links) per time point and lake and divided them by all the total possible bottom-up or top-down links for this network. Moreover, we averaged the strength of all significant bottom-up and top-down links per time point and lake. Then we calculated the difference between realized top-down and bottom-up links (i.e. top-down connectance - bottom-up connectance) and top-down and bottom-up strength (i.e., top-down interaction strength - bottom-up interaction strength). This resulted in a time series of changes in top-down - bottom-up connectance and interaction strength over time, whereas a value > 0 indicated top-down and < 0 bottom-up control (**Fig. 3a-b**). If there were no significant bottom-up and/or top-down links at a given time point, connectance was set to 0 and strength to NA. **Interaction types.** We summed up all trophic, non-trophic and hybrid interactions (according to **Fig. 1c**) per time point and lake and divided them by all total possible links per interaction type. Then we averaged connectance and interaction strength for trophic, non-trophic and hybrid links per time point across lakes. This resulted in a time series of connectance (%) and interaction strength of trophic, non-trophic and hybrid links (**Fig. 4a-b**). We compared connectance (%) and strength of interaction types using a Kruskal-Wallis test, a non-parametric method for testing if samples originate from the same distribution (**Fig. 4c-d**).

Scenario exploration using multivariate S-maps

We used multivariate s-maps (locally weighted linear maps) to model network properties and extract their relationship with phosphate levels and water temperature. S-maps compute a unique locally weighted

linear regression to make a forecast at each point in time where closer points on the attractor are given a higher weight. The strength of weighting is controlled by the parameter theta and indicates the degree of non-linearity and state dependency. Each regression provides a set of coefficients that define relationships (dynamics) between variables at each unique state. These coefficients were used to estimate (predict) each network property at varying levels of temperature and phosphate (**Fig. 2-4 c-d**). To account for important differences in the morphometry of lakes, which influence these ecosystems' responses to changes in nutrient inputs and warming, we included depth at the sampling site and lake total water volume in the s-map models [35]. To generate model predictions for the smallest lake (**Fig. 2-4 c-d**), we used the depth and volume of Lake Greifensee and for the largest lake, the depth and volume of Lake Zurich. Predictions for the three other lakes (Baldegg, Hallwil and Sempach) are in **Supplementary**.

We ran s-map models using rEDM (**v-0.7.5)** and the function **block_lnlp**. Environmental drivers were smoothed within 60-month moving windows to match the temporal scale of modeled network properties. Methods within the function were set to “s-map” and the exclusion radius to 12 to avoid the high temporal autocorrelation caused by the moving windows. Theta was selected to maximise predictive skill rho when varied over a list of values (0, 0.0001, 0.0003, 0.001, 0.003, 0.01, 0.03, 0.1, 0.3, 0.5, 0.75, 1.0, 1.5, 2, 3, 4, 6, and 8) and tp set to 0.

Methods References

46. Mieleitner, J. & Reichert, P. Modelling functional groups of phytoplankton in three lakes of different trophic state. *Ecol. Modell.* **211**, 279–291 (2008).

47. Monchamp, M.-E. *et al.* Homogenization of lake cyanobacterial communities over a century of climate change and eutrophication. *Nat Ecol Evol* **2**, 317–324 (2018).

48. Monchamp, M.-E., Spaak, P. & Pomati, F. High dispersal levels and lake warming are emergent drivers of cyanobacterial community assembly in peri-Alpine lakes. *Sci. Rep.* **9**, 7366 (2019).

49. Pomati, F. *et al.* Challenges and prospects for interpreting long-term phytoplankton diversity changes in Lake Zurich (Switzerland). *Freshwater Biology* vol. 60 1052–1059 (2015).

50. Benincà, E. *et al.* Chaos in a long-term experiment with a plankton community. *Nature* **451**, 822–825 (2008).

51. van Someren Gréve, H., Kiørboe, T. & Almeda, R. Bottom-up behaviourally mediated trophic cascades in plankton food webs. *Proc. Biol. Sci.* **286**, 20181664 (2019).

52. Takens, F. Detecting strange attractors in turbulence. in *Dynamical Systems and Turbulence, Warwick 1980* 366–381 (Springer Berlin Heidelberg, 1981).

53. Sugihara, G. & May, R. M. Nonlinear forecasting as a way of distinguishing chaos from measurement error in time series. *Nature* **344**, 734–741 (1990).

54. Hsieh, C.-H., Glaser, S. M., Lucas, A. J. & Sugihara, G. Distinguishing random environmental fluctuations from ecological catastrophes for the North Pacific Ocean. *Nature* **435**, 336–340 (2005).

55. Sugihara, G., Grenfell, B. T., May, R. M. & Tong, H. Nonlinear forecasting for the classification of natural time series. *Philosophical Transactions of the Royal Society of London. Series A: Physical and Engineering Sciences* **348**, 477–495 (1994).

56. Anderson, C. N. K. *et al.* Why fishing magnifies fluctuations in fish abundance. *Nature* **452**, 835–839 (2008).

57. Sugihara, G. *et al.* Are exploited fish populations stable? *Proceedings of the National Academy of Sciences of the United States of America* vol. 108 E1224–5; author reply E1226 (2011).

58. Ye, H. & Sugihara, G. Information leverage in interconnected ecosystems: Overcoming the curse of dimensionality. *Science* **353**, 922–925 (2016).

59. Ye, H. *et al.* Equation-free mechanistic ecosystem forecasting using empirical dynamic modeling. *Proc. Natl. Acad. Sci. U. S. A.* **112**, E1569–76 (2015).

60. Dixon, P. A., Milicich, M. J. & Sugihara, G. Episodic fluctuations in larval supply. *Science* **283**, 1528–1530 (1999).

61. Chang, C.-W., Ushio, M. & Hsieh, C.-H. Empirical dynamic modeling for beginners. *Ecol. Res.* **32**, 785–796 (2017).

62. Sommer, U. *et al.* Beyond the Plankton Ecology Group (PEG) Model: Mechanisms Driving Plankton Succession. (2012) doi:10.1146/annurev-ecolsys-110411-160251.

Figures

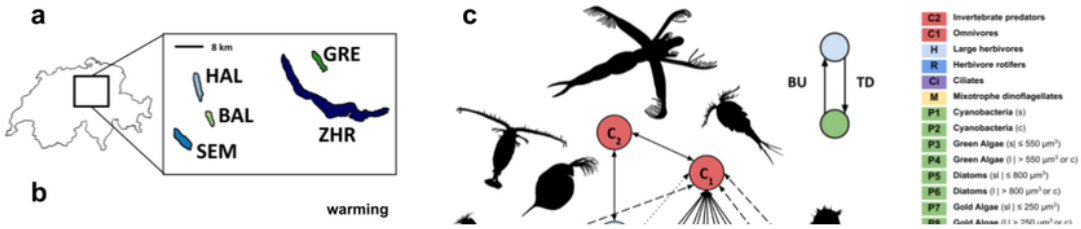

Figure 1

Environmental change in five Swiss lakes over the past five decades and its implications for plankton networks. [a] Study sites: Lake code names stand for HAL (Hallwil), BAL (Baldegg), SEM (Sempach), GRE (Greifen) and ZHR (Zurich). Lakes belong to the same geographic region, and the size and distance between them are to scale. **[b]** Monthly phosphate concentrations (PO_4) and water temperature data averaged over the water column: blue lines represent time series for single lakes, the black line represents

a smoothing average across lakes; dashed vertical lines indicate transitions in the lakes' histories, i.e., the end of the oligotrophication phase (circa the year 2000), and the increase in net lake warming (from circa 2010). **[c]** Conceptual model of a plankton network in temperate lakes: in the legend, (s) stands for small single cells, (l) for large single cells, and (c) for colonial taxa). Non-trophic links encompass facilitation and competition. Trophic links represent predator-prey interactions. Hybrid links can be both trophic and non-trophic, e.g., mixotrophic protists can prey on or compete with other phytoplankton species. Hybrid and trophic links go from the bottom to the top of the food web, i.e., from a primary producer to a grazer (bottom-up - BU) or from top to bottom, i.e., from a grazer to a primary producer (top-down - TD).

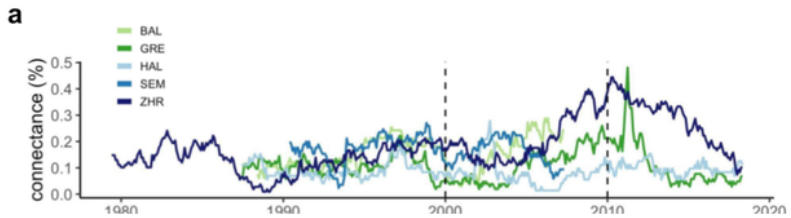

Figure 2

Connectance and interaction strength between the nodes of plankton networks are dynamic and exhibit non-linear relationships with water temperature and phosphorus. [a] Connectance (% realized network links across time); **[b]** average interaction strength between guilds across time (lines are drawn based on the center point of a moving window of 60 months - used for causality detection via CCM). **[c]** Combined effects of average water-column phosphate levels and temperature on realized connectance and **[d]**

average interactions strengths: color-coded contour plots depict the s-map model inferred relationships, which emerge from predicting network properties (Z-axis) over varying levels of the chosen pair of explanatory variables (water temperature and phosphate), across the entire dataset while keeping lake depth and volume constant (Methods). To model the smallest and largest lake, we used lake depth and volume from Greifensee and lake Zurich, respectively (other lakes in Supplementary). Water temperature (y-axis), phosphate levels (x-axis), connectance (legend c) and average interaction strength (legend d) ranged between the minimum and maximum observed value across all lakes. Dots depict the start/end of the re-oligotrophication and net-warming phase. Trajectories show the direction of time, for Greifensee (small lake) and Zurich (large lake), with the arrowhead pointing to the end of each phase. The displayed year is the middle point of a 5-year time window. Upwards triangles represent the maximum value of connectance or strength measured for paired values of water temperature and phosphate, whereas downwards triangles indicate the minimum.

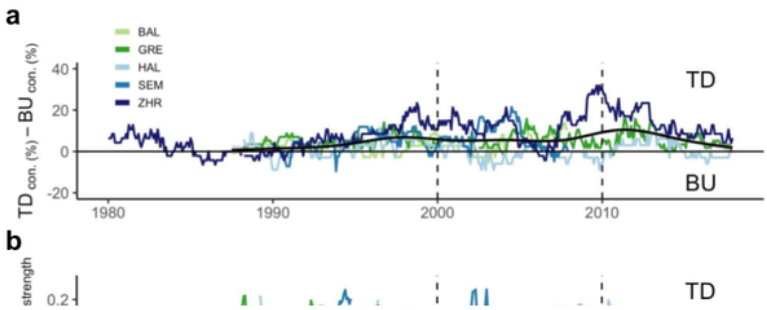

Figure 3

Warming reduces the number and strength of top-down (TD) relative to bottom-up (BU) network links. [a] Difference between amount of realized TD and BU links and **[b]** difference between the strength of TD and BU links: positive values mean more TD links, while negative values indicate more BU links; smoothing line shows a trend of TD vs. BU controls, and all lines are drawn based on the center point of a moving window of 60 months, used for causality detection via CCM. **[c-d]** Combined effects of average

water-column phosphate levels and temperature on realized TD and BU links **[c]**, and the difference between the strength of TD and BU links **[d]**: color-coded contour plots depict the s-map model inferred relationships across the entire dataset while keeping lake depth and volume constant (see **Fig. 2** and Methods).

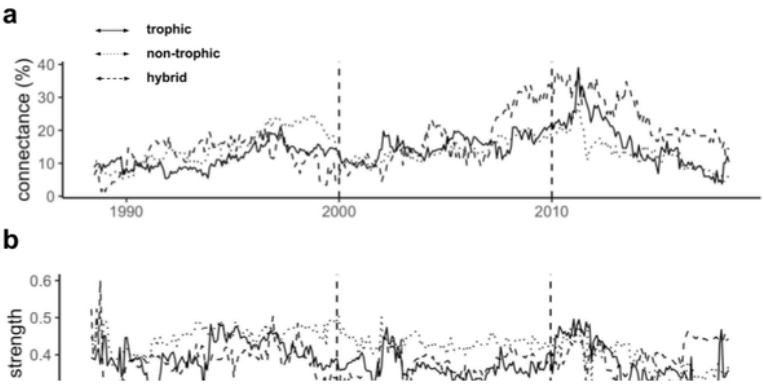

Figure 4

Hybrid links are conspicuous at the onset of lake warming, while non-trophic interactions are strongest during re-oligotrophication [a] Temporal changes in realized connectance (%) and **[b]** strength of trophic, non-trophic and hybrid interactions: all lines are drawn based on the central point of a moving window of 60 months, used for causality detection via CCM. **[c]** Prevalence and **[d]** Strength of trophic, non-trophic and hybrid links: points represent averages over time within lakes; boxes encompass all links across lakes during the whole studied period, whereas the lower and upper hinges correspond to the first and third quantiles (the 25th and 75th percentiles); P-values were calculated using pairwise comparisons and a Kruskal-Wallis test.

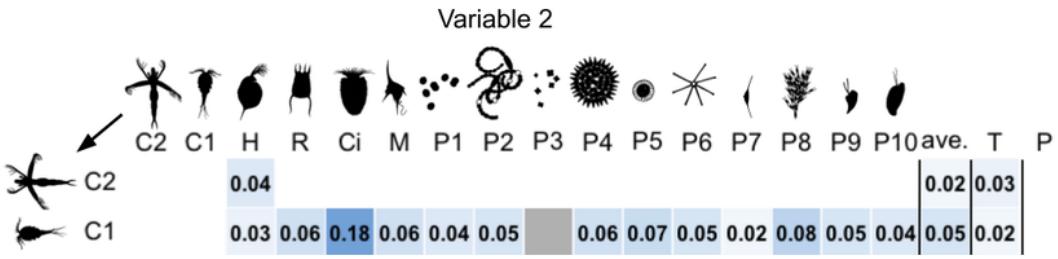

Figure 5

Small grazers and colonial cyanobacteria are the most strongly connected guilds in the network. Interaction strengths were calculated by multiplying the average strength (rho, corrected for seasonality) by its prevalence (i.e., if a link was significant within 50% of time windows, prevalence would be 0.5). The direction of the interaction is Variable 2 → Variable 1. Ave. is the average interaction strength for each guild. T is water temperature and P is phosphate levels. White tiles are interactions not occurring based

on the conceptual network (**Fig. 1 c**) and gray tiles are interactions that were not significant in none of the lakes based on a convergence test in CCM.

Supplementary Files

This is a list of supplementary files associated with this preprint. Click to download.

- supplementarymaterials.docx